The nature of attractors in an asymmetric spin glass with deterministic dynamics

1988 J. Phys. A: Math. Gen. 21 2775

(http://iopscience.iop.org/0305-4470/21/12/020)

J. Phys. A: Math. Gen. **21** (1988) 2775-2797. Printed in the UK

The nature of attractors in an asymmetric spin glass with deterministic dynamics

H Gutfreund†, J D Reger‡ and A P Young‡

† Physics Department, Hebrew University, Jerusalem, Israel
‡ Physics Department, University of CAlifornia, Santa Cruz, CA 95064, USA

Received 15 October 1987

Abstract. We study the attractors in an infinite-range Ising spin-glass model with deterministic dynamics where the interactions have asymmetry, specified by a parameter k. We find a duality relation between the attractors for models with asymmetry parameters k and $1/k$. The attractors are fixed points or limit cycles of short length, except for $k = 1$, at which the average cycle length diverges, reminiscent of a phase transition, and the model has many similarities to the random map model, as well as to the infinite-range symmetric spin glass in thermal equilibrium, including the fact that a few attractors dominate the weight. The extent of this dominance varies from sample to sample and so is given by a non-trivial probability distribution, $\Pi(Y)$, which we compute numerically.

1. Introduction

There has recently been a growing interest in the properties of Ising systems with asymmetric interaction bonds (Hertz *et al* 1987, Crisanti and Sompolinsky 1987). This was mainly motivated by the study of neural network models (Little 1974, Hopfield 1982, Amit *et al* 1987) in which the dynamics of the network is represented as a flow in the space of Ising spin configurations. When the synaptic junctions between two neurons are symmetric, i.e. $J_{ij} = J_{ji}$, this flow can be described as a relaxation of a global energy function. This leads to an energy landscape of local minima (fixed points) in configuration space surrounded by valleys (basins of attraction). Since in biological systems $J_{ij} \neq J_{ji}$, it is of interest to investigate the effect of such an asymmetry on the dynamical evolution of the spin configurations. As soon as the asymmetry becomes non-zero there is no longer a monotonically decreasing energy, so limit cycles occur as well as fixed points. For parallel dynamics this happens also in the symmetric case, as explained below. In principle, chaotic behaviour can also appear. Since the number of states in the configuration space is finite (for a finite number of spins) all cycles have a finite length, but extremely long cycles would appear chaotic on any reasonable timescale. From the point of view of dynamical systems theory, these are therefore interesting models, having many degrees of freedom, in which to study the nature of the attractors.

In the present paper, we study the structure of flows in configuration space in an asymmetric spin-glass model with *deterministic* dynamics. We consider a system of N spins, *fully connected* by an interaction of the form

$$J_{ij} = J_{ij}^{S} + kJ_{ij}^{A} \tag{1.1}$$

0305-4470/88/122775+23$02.50

where $J_{ij}^{S} = J_{ji}^{S}$ and $J_{ij}^{A} = -J_{ji}^{A}$. The elements of the symmetric and antisymmetric matrices, J^{S} and J^{A}, are random independent Gaussian variables with zero mean and mean square equal to $J^2/[N(1+k^2)]$. The parameter k is a measure of the asymmetry. For $k=0$ the system reduces to the ordinary symmetric infinite-range Sherrington-Kirkpatrick (1975) model, and the $k=\infty$ limit yields a totally antisymmetric interaction. The case of $k=1$ corresponds to a fully asymmetric model in which the values of J_{ij} and J_{ji} are uncorrelated. For all other values of k there is a finite correlation between the interaction in the two directions

$$\langle J_{ij} J_{ji} \rangle = \frac{J^2}{N} \frac{1-k^2}{1+k^2} \tag{1.2}$$

where $\langle \ldots \rangle$ denotes an average over the J_{ij}.

Our analysis is restricted to the following two types of dynamics.

(a) Parallel dynamics. All the spins are updated simultaneously at discrete time steps. The 'new' values $S(t+1)$ are determined by the 'old' ones, $S(t)$, through

$$S_i(t+1) = \operatorname{sgn}\left(\sum_j J_{ij} S_j(t) \right) \tag{1.3}$$

where the Ising spins $S_i(t)$ take values ± 1.

(b) Sequential dynamics. The spins are updated one after the other in a fixed order, which does not change from one round of updating the whole system to the next. If $S_i(t)$ is the configuration obtained after a sweep through the whole system has been completed, then the values $S_i(t+1)$ after the next round of updating are given by

$$S_i(t+1) = \operatorname{sgn}\left(\sum_{j<i} J_{ij} S_j(t+1) + \sum_{j>i} J_{ij} S_j(t) \right). \tag{1.4}$$

The index j now determines the order of updating.

These two types of dynamics are deterministic, which means that every initial configuration evolves to a definite attractor, which can be either a single stationary configuration (fixed point) or a periodic repetition of l configurations (cycle of length l). Thus, the dynamical process divides the configuration space into separate basins of attraction.

Let us define a weight of the sth basins of attraction as

$$W_s = \Omega_s / 2^N \tag{1.5}$$

where Ω_s is the total number of initial configurations which flow to the sth attractor. Note that we do *not* weight the states by any factor involving their energy, as one would do in statistical mechanics. A quantity of interest, which characterises the structure of the 'multivalley' landscape of the basins of attraction, is

$$Y = \sum_s W_s^2. \tag{1.6}$$

If $Y \to 0$ as $N \to \infty$, this means that in the thermodynamic limit the landscape is dominated by increasingly many basins with weights which become smaller and smaller. On the other hand, if Y remains finite as $N \to \infty$, it means that there are a few large basins of attraction which cover almost the whole configuration space. Another question of interest is if Y is independent of the particular realisation of the J_{ij} as

$N \to \infty$, i.e. if Y is self-averaging, or if it fluctuates from sample to sample. This happens if $\langle Y^2 \rangle - \langle Y \rangle^2 \neq 0$ as $N \to \infty$. In this case, the entire information on the statistics of the sizes of the basins of attraction is contained in $\Pi(Y)$, the probability distribution of Y.

These properties have been studied recently for several systems of interest in physics, biology, optimisation and mathematics. Let us mention three examples.

(i) The mean field theory of an infinite-range spin glass (Mézard *et al* 1984). This system is characterised by the existence of a large number (infinite when $N \to \infty$) of almost degenerate equilibrium states associated with free energy valleys separated by free energy barriers which become infinitely high in the thermodynamic limit. To each equilibrium state one can assign a weight $W_s \propto \exp(-F_s/T)$, where F_s is the free energy of the state.

(ii) The random map model (Derrida and Flyvbjerg 1987a) and the Kauffman model (Derrida and Flyvbjerg 1986). In this model the dynamical flow in configuration space is determined by a random mapping which uniquely assigns to each configuration its immediate successor. The interest in this model is twofold. First, many of the statistical properties of the basins of attraction and of the sizes of the attractors are known analytically. Second, this model is a limiting case of a class of Kauffman models which have been proposed and studied in the context of models for prebiotic evolution (Kauffman 1969, 1984). In the Kauffman models $S_i(t+1)$ is determined by a random Boolean function of the values of $S_j(t)$ on K randomly chosen sites. The random-map model is obtained when $K \to \infty$.

(iii) Random breaking of intervals (Derrida and Flyvbjerg 1987b). This is another model in which a definite algorithm determines the breaking of a system into an infinite number of separate pieces. The weights are in this case defined as the lengths of the broken intervals. This model is conceptually simple, and it was studied recently to demonstrate that it has many striking similarities with the other two models (Derrida and Flyvbjerg 1987b).

Although these models appear to be very different, they have many common features. In all of them, the phase space is divided into infinitely many valleys, but the weights of the largest valleys remain finite as $N \to \infty$, and they fluctuate from sample to sample. Moreover, the probability distribution $\Pi(Y)$ shows some 'universal' features which are found in the three models.

In the present paper we demonstrate that the asymmetric spin glass with deterministic dynamics and $k = 1$ falls into the same class of models, and we show how these unique properties build up when $k \to 1$ from both sides. We study the number and size of the attractors for arbitrary k and obtain an interesting 'duality' relation between the properties of the attractors for asymmetry factors k and $1/k$. Perhaps surprisingly, the model is not very chaotic, the dominant attractors are fixed points or short cycles (of length 2 or 4), except for $k = 1$ where the average cycle length diverges.

Our analysis is based on tracing the flow of all the configurations in a small system (up to $N = 16$). In § 2 we explain the method and demonstrate that one can derive reliable conclusions from the analysis of small systems. In § 3 we discuss the effect of the asymmetry parameter k on the lengths of the attractors and on the sizes and numbers of their basins of attraction, and we conclude that $k = 1$ is a unique transition point. In § 4 we study the statistical properties of the distribution function $\Pi(Y)$ and of its moments in the case of $k = 1$, and compare the results with the models mentioned above. Our results are summarised in § 5 and some technical details are collected in the appendices.

2. Analysis of small systems

We study the statistical properties of the dynamical landscape of the model defined in the introduction by analysing the evolution of every configuration and computing all the attractors and their basins of attraction for each sample. We can do this for $N \leqslant 16$. We first generate the interaction matrix defined in equation (1.1) and then compute for each configuration its immediate successor (obtained after one time step in parallel dynamics or after updating all the spins in sequential dynamics). The 2^N values of the 'next-state' configurations define the dynamical structure of the configuration space. This structure can be depicted graphically by points representing the configuration, connected by arrows indicating the transitions. A typical example is shown in figure 1. Each cluster of points defines a basin of attraction. By analysing the structure implied by such 'next-state' vectors we can compute the number and size of the attractors and of their basins. An outline of the algorithm which does this is given in appendix 2. To obtain good statistics we sample a large number of different realisations of the J_{ij}. We also calculate the weights of the basins of attraction defined in equation (1.5), their moments

$$Y_n = \sum_s W_s^n \tag{2.1a}$$

their corresponding averages

$$\langle Y_n \rangle = \left\langle \sum_s W_s^n \right\rangle \tag{2.1b}$$

and the moments $\langle Y_n^m \rangle$ defined by

$$\langle Y_n^m \rangle = \left\langle \left(\sum_s W_s^n \right)^m \right\rangle. \tag{2.1c}$$

By convention Y without a subscript will mean Y_2. Calculating Y for many samples also allows us to obtain directly the probability distribution $\Pi(Y)$.

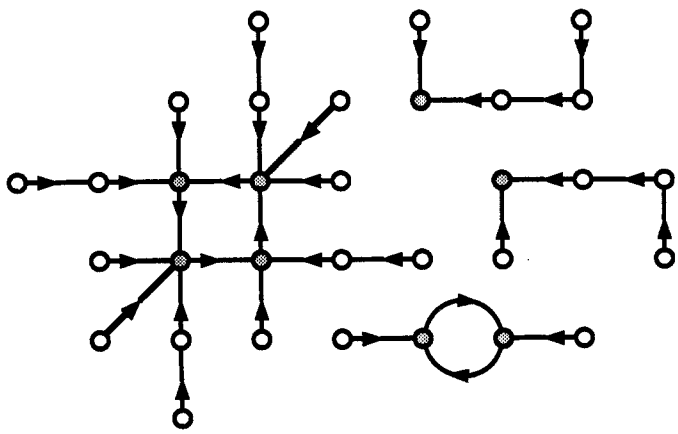

Figure 1. Example of the phase space for $N = 5$ spins, obtained by parallel dynamics for asymmetry parameter $k = 1.0$. There are four basins of attraction. The attractors (shaded) are: two fixed points, one 2-cycle and one 4-cycle.

To calculate these quantities for large systems one has to apply a stochastic approach. For example, Y_n can be obtained by counting the number of times that, in a given sample, n randomly chosen initial configurations fall onto the same attractor. This has then to be averaged over many samples to get $\langle Y_n \rangle$. The second moment $\langle Y^2 \rangle$ can be computed as the average number of times that, out of four configurations chosen at random, two will flow to attractor A and the other two to a different attractor B. These methods become very costly when n increases and have been used previously to calculate only the lowest moments (Derrida and Flyvbjerg 1986). It does not seem feasible to use them to compute very high moments or quantities such as the total number of attractors. This is the reason why we decided to use exhaustive enumeration of all trajectories in configuration space for small systems.

Of course the question arises as to whether the results obtained for systems of size $N \leqslant 16$ can be used to derive the behaviour in the thermodynamic limit. It seems that this is indeed the case as far as the number and length of the attractors is concerned. To demonstrate this, we present in § 2.1 numerical results for the number of fixed points and compare them with the known analytical values. For the other quantities studied in this paper the situation is somewhat different. In the random map model all the known features of an infinite system are quantitatively reproduced already for $N \simeq 12$. This is shown in § 2.2. In our model at $k = 1$ the analysis of small systems reproduces the qualitative features of large systems and allows us to make analogies with other models and to emphasise the distinction from the behaviour for k different from 1. However, the calculated quantities themselves do not yet converge to their thermodynamic limit. This will be discussed in § 4.

2.1. The number of fixed points

A stationary configuration $\{S_i\}$, stable to a single spin flip, satisfies the condition

$$\sum_j J_{ij} S_j = \lambda_i S_i \qquad \lambda_i > 0 \qquad i = 1, 2, \ldots, N. \tag{2.2}$$

The average number of configurations which satisfy the condition can be calculated from

$$\langle N_1(k) \rangle = \left\langle \mathrm{Tr} \int_0^\infty \prod_i \mathrm{d}\lambda_i \, \delta\left(\sum_j J_{ij} S_j - \lambda_i S_i \right) \right\rangle \tag{2.3}$$

where the trace is taken over the spins. Note that the condition (2.2) does not depend on the type of dynamics used. Thus, the number of fixed points will be the same for both types of dynamics considered here and also for random sequential updating. The right-hand side of equation (2.3) was first calculated by Tanaka and Edwards (1980) for the symmetric case, and their calculation can easily be extended to the asymmetric J_{ij} given by equation (1.1) (see appendix 1). Similar results were also obtained by Sompolinsky (1987) and Bray (1987). For large N, the result can be written in the form

$$\langle N_1(k) \rangle = A(k) \exp(N\alpha_1(k))[1 + \mathrm{O}(1/N)] \tag{2.4}$$

where

$$\alpha_1(k) = -\frac{\omega^{*2}}{2} + \ln\left\{ 1 + \mathrm{erf}\left[\left(\frac{(1-k^2)}{2(1+k^2)} \right)^{1/2} \omega^* \right] \right\} \tag{2.5}$$

and ω^* is defined by the equation

$$\omega^* = \left(\frac{2(1-k^2)}{\pi(1+k^2)}\right)^{1/2} \exp\left(-\frac{(1-k^2)}{2(1+k^2)}\omega^{*2}\right)\left\{1+\operatorname{erf}\left[\left(\frac{(1-k^2)}{2(1+k^2)}\right)^{1/2}\omega^*\right]\right\}^{-1} \tag{2.6}$$

where erf denotes the error function. An expression for the coefficient $A(k)$ is given by equation (A1.11) in appendix 1. Throughout this paper, when we discuss attractors of a given length, the subscripts on $\alpha(k)$ and $N(k)$ refer to the length of the attractor and $\alpha_i(k)$ will always be the coefficient of N in the exponent for the corresponding $\langle N_i(k)\rangle$. Where the subscript is 'tot' we are referring to the total number of attractors.

We have calculated the number of fixed points for even values of N between $N=4$ and $N=16$. In figure 2 we plot the results for $k=0$ and $k=0.5$. The numbers for the largest sizes were obtained by averaging over several hundred samples and the smaller ones over several thousands. One observes that even for the small systems the results fall close to a straight line. From these plots we can derive values of the exponent $\alpha_1(k)$ and the coefficient $A(k)$. For example, the exact values of $A(k)$ for $k=0$ and $k=0.5$ are 1.051 and 1.023, respectively. We find 1.065 and 1.015. Our numerical values of the exponent are compared with the theoretical curve for $\alpha_1(k)$ in figure 3. The agreement is evidently very good.

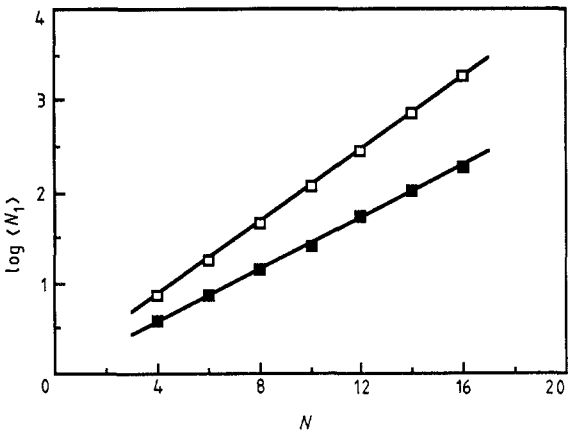

Figure 2. Logarithm of the average number of fixed points, $\langle N_1\rangle$, plotted against system size for asymmetry parameter values $k=0.0$ (□) and $k=0.5$ (■). From the slopes we find $\alpha_1(k=0)=0.198$ and $\alpha_1(k=0.5)=0.141$.

Of particular interest is the case $k=1$. The integrals in appendix 1 can be evaluated exactly, without needing the steepest descents approximation, and one finds

$$\langle N_1(k=1)\rangle = 1 \tag{2.7}$$

for all sizes. This result is confirmed by our numerical calculations. An alternative derivation of it, and a discussion of its significance, will be given in § 3.3.

It is interesting to ask whether $\langle N_1(k)\rangle$ could be dominated by a few rare samples, in which case self-averaging would not occur, i.e. $\langle \log N_1(k)\rangle \neq \log(\langle N_1(k)\rangle)$ even for $N\to\infty$. To check this possibility we computed $\langle \log N_1(k)\rangle$ as well as $\log(\langle N_i(k)\rangle)$. We find that they agree well with each other, e.g. for $k=0$ and the largest sizes the difference is less than 1%. As $k\to 1$, where N_1 is small, the difference is bigger but still decreases with increasing system size, so one has to go to larger system sizes to see the self-

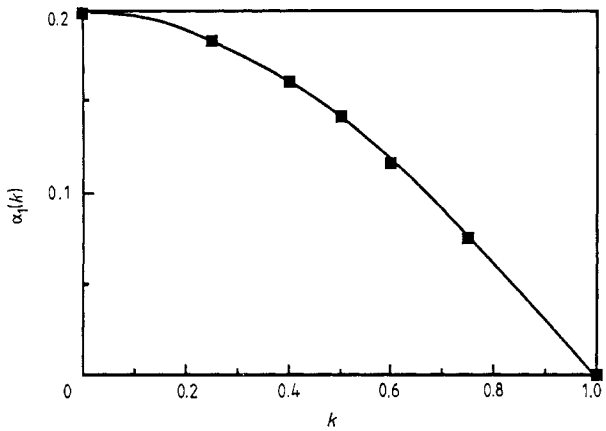

Figure 3. Numerical results for α_1 (■) as a function of the asymmetry parameter k, compared with the theoretical curve obtained from equation (2.5) of the text.

averaging. We conclude that the number of fixed points is self-averaging for $0 \leqslant k < 1$. It cannot be self-averaging for k precisely equal to 1 because $\langle N_1 \rangle = 1$ from equation (2.7), whereas each sample must have an *even* number of fixed points because of the symmetry of the Hamiltonian under the transformation $S_i \to -S_i$, for all i.

2.2. The random map model

In this model phase space is composed of M states and the dynamics is just a random map: for each state one chooses at random another state to be its immediate successor. In this model, one can compute exactly the quantities $\langle Y_n \rangle$ and the moments $\langle Y_n^m \rangle$. We have calculated several of these quantities for different system sizes $M = 2^N$. The results are given in table 1. For $N \geqslant 12$, they compare very well with the exact values.

Another quantity which can be easily calculated is the probability distribution, $\Pi(Y)$. In figure 4 we show the result for $N = 12$ (averaged over 36 000 samples) and compare it with the curve obtained by Derrida and Flyvbjerg (1987a) by an indirect and more elaborate method. Again the agreement is excellent.

We presented these results to illustrate that there is a model in which small sizes describe well the behaviour for $N \to \infty$. We shall see that this is not true to the same

Table 1. Comparison of the exact values (as $M \to \infty$) of various moments of the weights in the random map model with the numerical results for different sizes $M = 2^N$. The number of samples is shown in brackets.

	Exact $N \to \infty$	$N = 8$ (80 000)	$N = 10$ (51 000)	$N = 12$ (36 000)	$N = 14$ (26 000)	$N = 16$ (20 000)
$\langle Y_2 \rangle$	0.666	0.680	0.675	0.669	0.668	0.669
$\langle Y_3 \rangle$	0.533	0.550	0.545	0.537	0.535	0.537
$\langle Y_4 \rangle$	0.457	0.476	0.470	0.461	0.459	0.461
$\langle Y_2^2 \rangle$	0.495	0.514	0.507	0.499	0.497	0.499
$\langle Y_2^3 \rangle$	0.398	0.419	0.412	0.403	0.400	0.402

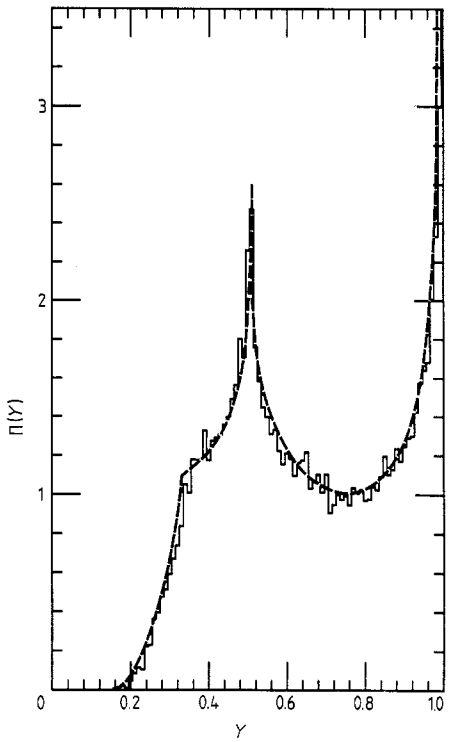

Figure 4. Histogram of the numerical results for the probability distribution $\Pi(Y)$ in the random map model. The system size is $N = 12$. The broken curve is from Derrida and Flyvbjerg (1987a).

extent for the asymmetric spin glass at $k = 1$, although both models have similar behaviour in the $N \to \infty$ limit.

3. Structure of attractors as a function of asymmetry parameter

In this section we discuss how the number of attractors and the corresponding cycle length varies with the asymmetry parameter k.

The number of fixed points, which is of course the same for sequential and parallel dynamics, has already been discussed in § 2.1. For $0 < k < 1$, $\langle N_1(k) \rangle$ increases exponentially with N, while for $k = 1$, $\langle N_1(1) \rangle = 1$, and finally, if $k > 1$, $\langle N_1(k) \rangle$ decreases exponentially with N. The variation of α_1 with k was shown in figure 3. Now we discuss cycles for which it is necessary to distinguish between sequential and parallel dynamics. First of all we shall describe our results for sequential dynamics.

3.1. Sequential dynamics

It is well known that there are only fixed points for $k = 0$. In the opposite extreme, for $k = \infty$, we can show that there are only limit cycles of length 2 by the following argument. The dynamics of the system is governed by equation (1.4). Let us modify

this, replacing J_{ij} by J'_{ij}, where

$$J'_{ij} = J_{ij} \qquad i > j \tag{3.1}$$

$$J'_{ij} = -J_{ij} \qquad i < j \tag{3.2}$$

and replacing $S_i(t)$ by $S'_i(t)$ where

$$S'_i(t) = S_i(t) \qquad t \text{ even} \tag{3.3}$$

$$S'_i(t) = -S_i(t) \qquad t \text{ odd.} \tag{3.4}$$

Then equation (1.4) has precisely the same form as before, but is written in terms of the primed variables, i.e.

$$S'_i(t+1) = \operatorname{sgn}\left(\sum_{j<i} J'_{ij} S'_j(t+1) + \sum_{j>i} J'_{ij} S'_j(t) \right). \tag{3.5}$$

Thus the dynamics for the sets of interactions J and J' are the same if we invert the spins at every alternate time when using J'. The transformation from J to J' effectively interchanges the two terms in equation (1.1) and thus changes an interaction with an asymmetry parameter k to one with $1/k$. We therefore see the following 'duality' relation between asymmetry parameters k and $1/k$: for every attractor with a given set of J_{ij} (which has asymmetry parameter k) there is a corresponding attractor for the set of J'_{ij} (which has asymmetry parameter $1/k$). Note that this relation holds separately for *each set of interactions* provided one updates with the J matrix and the J' matrix in the same order. Since the order of updating does not affect averaged quantities the duality property holds *statistically* even when the order of updating is different in the two cases. As a result of duality it follows, for example, that

$$\langle \tilde{N}^{\mathrm{s}}_2(k) \rangle = \tfrac{1}{2} \langle N_1(1/k) \rangle \tag{3.6}$$

where the tilde indicates that we only consider 2-cycles where the two states are inverses of each other, and the factor of $\frac{1}{2}$ is due to the fact that if state A is a fixed point, which implies that $-A$ is also a fixed point, they give the *same* 2-cycle under the duality transformation. In equation (3.6) and for the rest of this paper the superscript s refers to sequential dynamics. Since the number of attractors varies exponentially with N, one has

$$\tilde{\alpha}^{\mathrm{s}}_2(k) = \alpha_1(1/k) \tag{3.7}$$

and similar results can be derived for cycles of longer length. For $k = \infty$ there are only 2-cycles since fixed points are the only attractors for $k = 0$. Because of the exponential dependence on N the total number of attractors $\langle N^{\mathrm{s}}_{\mathrm{tot}} \rangle$ is just the number of those attractors with the largest α. Consequently,

$$\alpha^{\mathrm{s}}_{\mathrm{tot}}(k) = \alpha^{\mathrm{s}}_{\mathrm{tot}}(1/k) = \alpha_1(k) \qquad 0 \leqslant k \leqslant 1. \tag{3.8}$$

To test out these predictions we plot in figure 5 our results for $\alpha_1(k)$ and $\tilde{\alpha}^{\mathrm{s}}_2(1/k)$ for $0 \leqslant k \leqslant 1$, obtained by fits for $4 \leqslant N \leqslant 16$. The agreement is seen to be very good. Furthermore, it appears that the vast majority of attractors are fixed points for $k < 1$, and 2-cycles with states the inverses of each other for $k > 1$. To see this, we plot in figure 6(a) the remaining number of attractors (including 2-cycles where the states are *not* inverses of each other) and compare with the total number in figure 6(b). Note that the numbers in figure 6(a) are much smaller than those in figure 6(b) and also

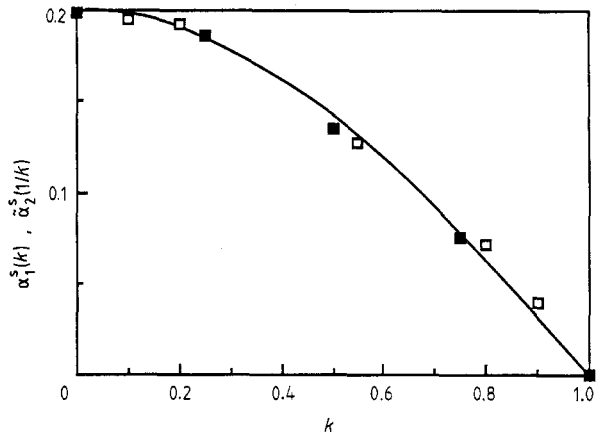

Figure 5. Plot of $\alpha_1^s(k)$ (■) and $\tilde{\alpha}_2^s(1/k)$ (□) against k for sequential dynamics, together with the theoretical curve for $\alpha_1(k)$ from equation (2.5).

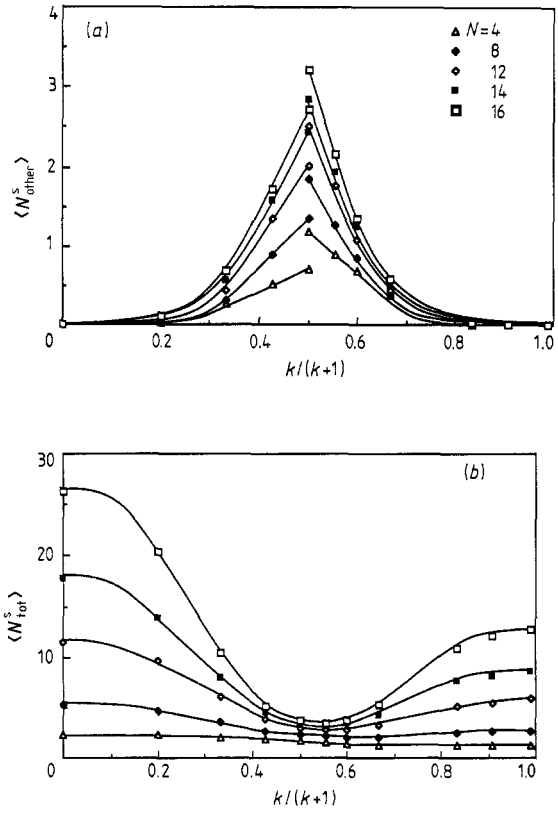

Figure 6. (*a*) Average number of attractors without the major contributions $\langle N^s_{other} \rangle$ in sequential dynamics plotted against the asymmetry parameter $k/(k+1)$. For $k<1$ we subtracted the number of fixed points from the total number of attractors, and for $k>1$ the number of 2-cycles in which the states are inverses of each other (mirror states). (*b*) The average total number of attractors $\langle N^s_{tot} \rangle$ plotted against $k/(k+1)$ for sequential dynamics.

that they increase slowly with N, probably less fast than exponential, though it is hard to rule out a small exponent.

Data for $k = 1$ are shown in figure 7 from which one deduces that

$$\langle N_{\text{tot}}^{s} \rangle = CN + D \qquad k = 1 \tag{3.9}$$

where $C \simeq 0.17$. This linear dependence on N is also found (Derrida and Flyvbjerg 1987a) for the random map model, with $C = 0.5$. Indeed, we shall emphasise in § 3.3 below that the spin glass with $k = 1$ is very similar, in many respects, to the random map model.

We have shown that there are an exponentially large number of attractors, except for $k = 1$, which marks a phase transition where a qualitative change in the type of attractors takes place. For $k < 1$ there are mainly fixed points but for $k > 1$ there are mainly 2-cycles. This phase transition analogy can be pushed further by studying the average attractor size $\langle l \rangle$ defined by

$$\langle l \rangle = \left\langle \frac{1}{N_{\text{tot}}} \sum_{s=1}^{N_{\text{tot}}} l_s \right\rangle \tag{3.10}$$

where l_s is the length of the sth attractor. Note that this definition gives equal weight to all attractors. One could also weight them by their domain of attraction W_l, i.e.

$$\langle l' \rangle = \left\langle \sum_{s=1}^{N_{\text{tot}}} W_s l_s \right\rangle \tag{3.11}$$

but this was not computed. Figure 8 shows $\langle l \rangle$ against $k/(1+k)$ with sequential dynamics for different sizes. Clearly this is small until k approaches unity, where it becomes very large as N increases. Note that under the duality transformation $k \to 1/k$, then $x = k/(1+k)$ goes to $1-x$, so we expect a symmetry about $x = \frac{1}{2}$, which is indeed observed in figure 8. For $k = 1$ it appears that $\ln\langle l \rangle = a + bN$ where $b \simeq 0.072$ as shown in figure 9. Note that for the random map model one has (Derrida and Flyvbjerg 1987a) the same N dependence but with $b = \frac{1}{2}\ln 2$.

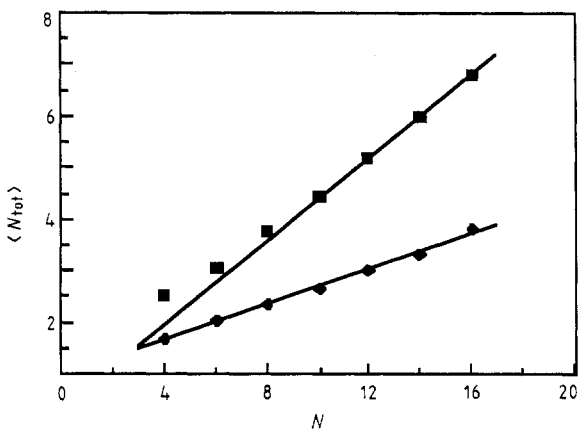

Figure 7. The average total number of attractors $\langle N_{\text{tot}} \rangle$ plotted against N for parallel (■) and sequential (◆) dynamics. The slopes are 0.41 and 0.17, respectively.

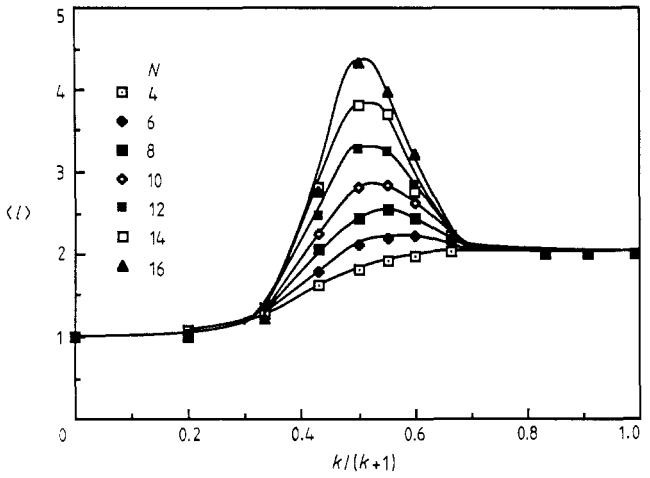

Figure 8. The average length of the attractors $\langle l \rangle$ against $k/(1+k)$ with sequential dynamics for different sizes.

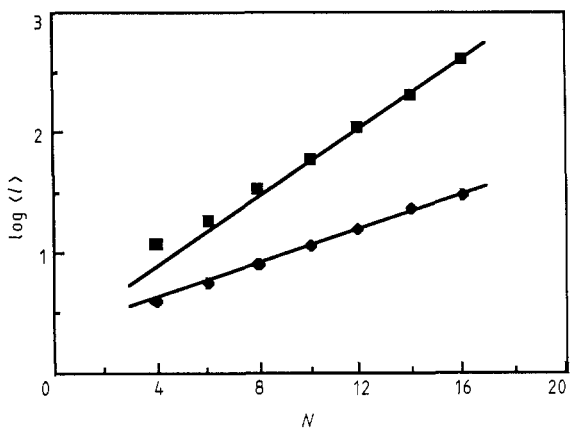

Figure 9. System size dependence of the average length of the attractors $\langle l \rangle$ for both parallel (■) and sequential (◆) dynamics. The slopes are 0.144 and 0.072, respectively.

3.2. *Parallel dynamics*

For parallel dynamics it has been shown (Goles-Chacc *et al* 1985) that there are only fixed points and 2-cycles for $k=0$. The technique can easily be generalised to show that there are only 4-cycles for $k=\infty$. Let us define an 'energy' $E(t)$ by

$$E(t) = -\sum_{\langle i,j \rangle} J_{ij} S_i(t) S_j(t-1). \tag{3.12}$$

Computing the difference $E(t+1)-E(t)$ one immediately finds, for J_{ij} symmetric ($k=0$), that

$$E(t+1)-E(t) = -\sum_i [S_i(t+1)-S_i(t-1)] \sum_j J_{ij} S_j(t). \tag{3.13}$$

Hence either $S_i(t+1) = S_i(t-1)$ for all i, which means one is on a fixed point or 2-cycle, or $E(t+1)-E(t)<0$, since $S_i(t+1) = \mathrm{sgn}(\Sigma\, J_{ij} S_j(t))$. Since the energy is bounded, it

must eventually stop decreasing so the system must end up on a fixed point or 2-cycle. If, on the other hand, J_{ij} is antisymmetric ($k=\infty$), one obtains

$$E(t+1)-E(t)=-\sum_i [S_i(t+1)+S_i(t-1)]\sum_j J_{ij}S_j(t) \tag{3.14}$$

instead of equation (3.13). Thus, either $E(t)$ decreases or $S_i(t+1)=-S_i(t-1)$ for all i. Hence, the only attractors are 4-cycles where the first and third states are inverses of each other, as are the second and fourth states, i.e. one has the sequence of states $A\to B\to -A\to -B\to A$.

For sequential dynamics we proved above a very general duality relation, which leads, for example, to equations (3.7) and (3.8). Unfortunately we have been unable to find as general a result for parallel dynamics, although the above discussion shows that there are analogous results connecting $k=0$ with $k=\infty$. Nonetheless, analytic calculations (Bray and Young 1987), making some plausible assumptions, show that, for arbitrary k, there is a simple relation between the number of 4-cycles with first and third states inverted and the number of 2-cycles for asymmetry parameter $1/k$, namely

$$\tilde{\alpha}_4^{\mathrm{p}}(1/k)=\alpha_2^{\mathrm{p}}(k) \tag{3.15}$$

which is clearly analogous to equation (3.7) for sequential dynamics. Here and from now on, the superscript p refers to parallel dynamics. The work of Bray and Young (1987) and our numerical results suggest that these 4-cycles dominate for $k>1$ and the 2-cycles dominate for $k<1$. If this is so then it follows that

$$\alpha_{\mathrm{tot}}^{\mathrm{p}}(k)=\alpha_{\mathrm{tot}}^{\mathrm{p}}(1/k). \tag{3.16}$$

Thus, there seems to be a duality for parallel dynamics similar to the one we derived for sequential dynamics, although we have been unable to give a general proof of it.

One can also show (Bray and Young 1987) that the number of 2-cycles is connected to the number of fixed points by the relation

$$\alpha_2^{\mathrm{p}}(k)=2\alpha_1(k) \qquad 0\leqslant k\leqslant 1 \tag{3.17}$$

which, combined with equation (3.15) and the remarks leading to equation (3.16), gives

$$\alpha_{\mathrm{tot}}^{\mathrm{p}}(k)=\alpha_{\mathrm{tot}}^{\mathrm{p}}(1/k)=2\alpha_1(k). \tag{3.18}$$

Equations (3.8) and (3.18) give the surprising result that the total number of attractors for any value of k, and for both sequential and parallel dynamics, is given by $\alpha_1(k)$ with k in the range $0\leqslant k\leqslant 1$.

These predictions are well confirmed by our results. Figure 10 shows that $\alpha_2^{\mathrm{p}}(k)$ and $\tilde{\alpha}_4^{\mathrm{p}}(1/k)$ agree well with the theoretical value of $2\alpha_1(k)$. The vast majority of attractors are indeed 2-cycles, for $0<k<1$, and 4-cycles with first and third states inverted for $k>1$, as can be seen from figure 11(a) which plots the number of attractors with these cycles (and for $k>1$ also the fixed points) removed. As for sequential dynamics the number increases slowly with N, probably less fast than exponential. Figure 11(b) shows the total number of attractors, which is clearly very much larger and is increasing much more rapidly with N. At $k=1$ we have $\langle N_{\mathrm{tot}}^{\mathrm{p}}\rangle = C'N+D'$, where $C'\simeq 0.41$ (see figure 7), which is reasonably close to the random map value of $\frac{1}{2}$. In fact, since there are deviations from the straight line fit in figure 7 at small sizes, we cannot rule out the possibility that C' is precisely equal to the random map value. We do not understand why there should be such a close correspondence between the random map model and the asymmetric spin glass with $k=1$. The logarithm of the

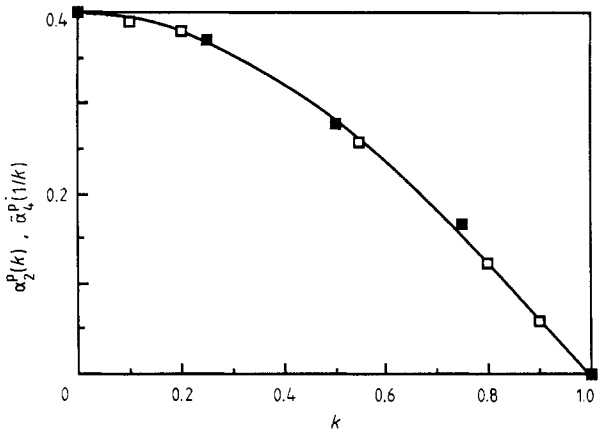

Figure 10. Plots of $\alpha_2^P(k)$ (■) and $\tilde{\alpha}_4^P(1/k)$ against k for parallel dynamics, together with the theoretical curve for $2\alpha_1(k)$.

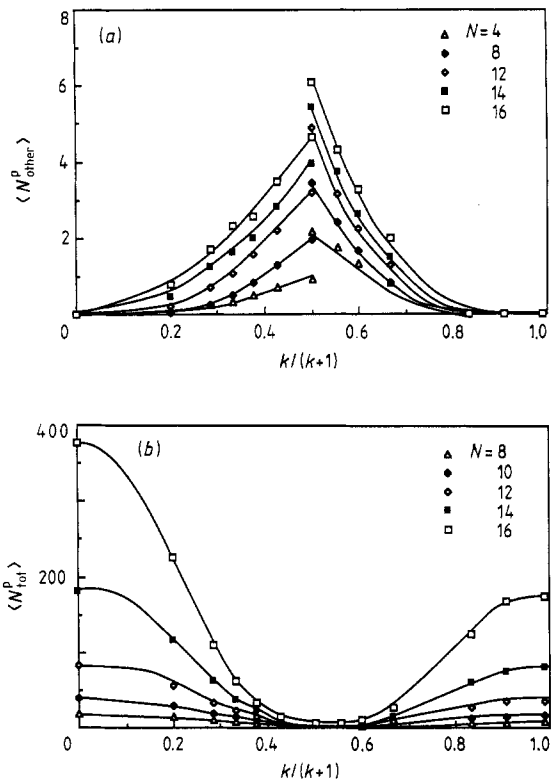

Figure 11. (*a*) Average number of attractors without the major contributions, $\langle N_{other}^P \rangle$, in parallel dynamics plotted against the asymmetry parameter $k/(k+1)$. For $k<1$ we subtracted the number of fixed points and 2-cycles from the total number of attractors, and for $k>1$ the number of 4-cycles in which the first and third states are inverses of each other (mirror states). (*b*) The average total number of attractors $\langle N_{tot}^P \rangle$ plotted against $k/(k+1)$ for parallel dynamics.

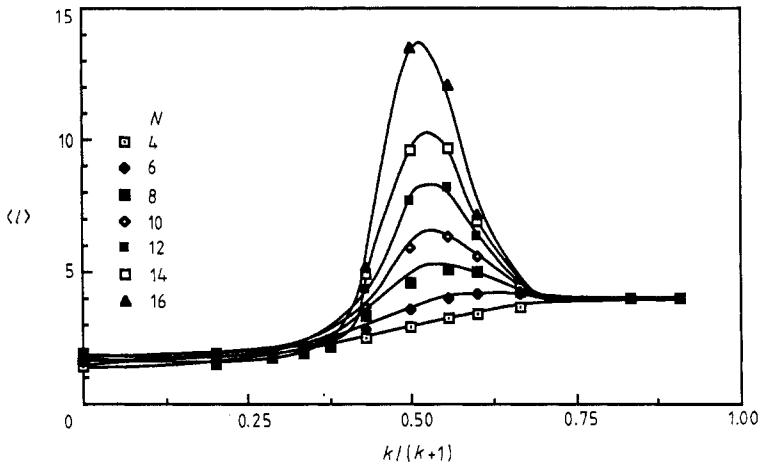

Figure 12. The average length of the attractors $\langle l \rangle$ against $k/(1+k)$ with parallel dynamics for different sizes.

average attractor size, shown in figure 9, varies as $a+bN$ with $b \simeq 0.144$. The N dependence is again the same as for the random map model (Derrida and Flyvbjerg 1987a) and our results for sequential dynamics given above, but the value of b is different. The average attractor size, $\langle l \rangle$, is plotted in figure 12. Like the corresponding data for sequential dynamics, presented in figure 8, this shows evidence for a phase transition at $k=1$.

3.3. Special behaviour at $k=1$

We now discuss the similarity between the spin-glass model at $k=1$ and the random map model. They both have the property that a configuration at time t goes with equal probability to any other configuration at time $t+1$. For the random map model, this follows trivially from the way the model is defined. To see that this is also the case for the spin-glass model, consider two configurations, $\{S_i\}$ and $\{S_i^0\}$. The probability that $\{S_i^0\}$ goes to $\{S_i\}$ in one time step is, in parallel dynamics, given by

$$P(S, S^0) = \left\langle \prod_i \Theta\left(S_i \sum_j J_{ij} S_j^0 \right) \right\rangle_J \tag{3.19}$$

where Θ is the step function. One can make a gauge transformation

$$J_{ij} = \varepsilon_i J'_{ij} \tag{3.20}$$

where $\varepsilon_i = \pm 1$. For $k=1$, and only for this value of k, J_{ij} and J_{ij} are uncorrelated so averaging over J_{ij} is equivalent to averaging over J'_{ij}. Thus

$$P(S, S^0) = \left\langle \prod_i \Theta\left(\varepsilon_i S_i \sum_j J'_{ij} S_j^0 \right) \right\rangle_{J'}. \tag{3.21}$$

Now $\varepsilon_i S_i = S'_i$ can be any configuration. Thus $P(S, S^0) = 2^{-N}$ for any S. The same argument can be applied in the case of sequential dynamics, when

$$P(S, S^0) = \left\langle \prod_i \Theta\left(S_i \sum_{j<i} J_{ij} S_j + S_i \sum_{j>i} J_{ij} S_j^0 \right) \right\rangle_J \tag{3.22}$$

except that now the interaction with $j>i$ are gauged as $J'_{ij} = \varepsilon_i J_{ij}$, and the rest as $J'_{ij} = \varepsilon_i \varepsilon_j J_{ij}$.

Since $P(S, S^0) = 2^{-N}$ for any S, one immediately finds that there is, on the average, one fixed point, because

$$\sum_{S^0} P(S^0, S^0) = 1. \tag{3.23}$$

Note, however, that this similarity does not imply that the two models are identical. Differences occur when one computes higher moments of the distribution of the quantity in equation (3.19). Such moments occur, for example, in the time evolution of the overlap of two initial configurations. Still there are some striking similarities between these models. For example the total number of attractors varies as $\langle N_{\text{tot}}^{\text{p}} \rangle = CN$ where $C = \frac{1}{2}$ for the random map model and $C \simeq 0.41$ for the spin glass with parallel dynamics. As discussed above, it is possible that the values of C are actually the same. We do not understand why the behaviour of these two models is so close.

To summarise the results of § 3, we have presented both numerical and analytic results which show that the number of attractors increases exponentially with N except for $k = 1$ where the number is proportional to N. The value $k = 1$ marks a transition at which there is a change in the nature of the dominant attractors. Only at this value of k is there a strong analogy with the other models discussed in the introduction. In the next section we explore further the connections between the spin glass with $k = 1$ and these other models.

4. The sizes of the basins of attraction

The statistical properties of the sizes of the basins of attraction are best characterised by the moments of their weights $\langle Y_n \rangle$ and by their fluctuations from sample to sample. These properties were first investigated for the infinite-range spin glass (Mézard *et al* 1984). Let us summarise the picture which emerges there.

The spin-glass phase is characterised by the existence of infinitely many equilibrium states (as $N \to \infty$). A state s may be described by the local magnetisations m_i^s. One can define an overlap between two equilibrium states, s and s', as

$$q^{ss'} = \frac{1}{N} \sum_i m_i^s m_i^{s'}. \tag{4.1}$$

For any given value of q, where $0 < q < 1$, one can divide the space of all the equilibrium states into clusters so that two states in the clusters have an overlap $q' > q$ and the overlap between states in different clusters is smaller than q. The weight of cluster I is defined as

$$W_I = \sum_{s \in I} P_s \tag{4.2}$$

where P_s is the Boltzmann weight of state s. The probability that two states have an overlap larger than q is

$$Y(q) = \sum_I W_I^2. \tag{4.3}$$

Even for $N \to \infty$ this quantity depends on the actual realisation of the J_{ij}. Furthermore, Y remains finite in this limit so the phase space is dominated by a small number of clusters of finite weight. It was shown (Mézard *et al* 1984) that the probability distribution $\Pi(Y)$ has a universal property; it depends on the temperature, the magnetic

field and the value of q only through the average $\langle Y\rangle$. The higher moments $\langle Y^n\rangle$ are just polynomials in Y. For example,

$$\langle Y^2\rangle = \tfrac{1}{3}(\langle Y\rangle + 2\langle Y\rangle^2) \tag{4.4}$$

$$\langle Y^3\rangle = \tfrac{1}{15}(3\langle Y\rangle + 7\langle Y\rangle^2 + 5\langle Y\rangle^3). \tag{4.5}$$

One can show directly (Mézard *et al* 1985) in the SK model or in the random energy model (Derrida and Toulouse 1985) that the quantities $\langle Y_n\rangle$ are also polynomials in $\langle Y\rangle$. For example,

$$\langle Y_3\rangle = \tfrac{1}{2}(\langle Y\rangle + \langle Y\rangle^2) \tag{4.6}$$

$$\langle Y_4\rangle = \tfrac{1}{6}(2\langle Y\rangle + 3\langle Y\rangle^2 + \langle Y\rangle^3). \tag{4.7}$$

Derrida and Flyvbjerg (1987a) observed from numerical calculations on the Kauffman (1984) model for several small values of the parameter K that such relations are approximately satisfied in that model for finite values of N. The fact that this is not exact can be inferred from the random map model. Using the values in the first column of table 1, one sees, however, that the discrepancy is very small. For example, the difference between the two sides of equation (4.4) is 0.023.

This similarity may come as a surprise. The mechanism of breaking up the phase space into separate 'valleys' in the SK model and the Kauffman models is different and so is the definition of the weights. Nevertheless, there are fundamental similarities in the nature of this multivalley structure.

In view of the above, we have checked numerically if relations (4.4)-(4.7) are also satisfied in our model. Our results for $N = 16$ and parallel dynamics are summarised in figures 13(a)-(d). For $k = 1$, these relations are satisfied at least as well as in the random map model. In each case, the points representing the different values of k lie on a trajectory which approaches the theoretical line when k increases towards $k = 1$. When k increases further, the points retreat from the theoretical curve along the same line. This may be related to the duality property in the structure of the attractors discussed in § 3. For $k = 1$ we find that, although the different quantities $\langle Y_n\rangle$ and $\langle Y^n\rangle$ have not yet saturated to their limiting values for $N = 16$, the proximity of the points to the theoretical curve does not depend much on N, as is demonstrated for parallel dynamics in figure 14 for relation (4.4). On the other hand, the size dependence for $k \neq 1$ is much stronger and the results move away from the full line as N varies from 4 to 16. The proximity to the theoretical line and the different size dependence indicates that as $N \to \infty$ the multivalley structure in the $k = 1$ case is very different from $k \neq 1$.

Another feature observed by Derrida and Flyvbjerg (1987b), which is common to all the models considered by them, is the presence of singularities in the distribution function $\Pi(Y)$ at the points $Y = 1/n$ where $n = 2, 3, \ldots$. These singularities become weaker and weaker as n increases and it is very hard to see them in numerical calculations for $n > 3$. Their origin and nature has been discussed in great detail for the model of random breaking of intervals (Derrida and Flyvbjerg 1987b), but their occurrence seems to be much more general. Incidentally, the curves of $\Pi(Y)$ in Mézard *et al* (1984), which were calculated from the first seven moments, do not show these singularities, and they appear only in a more rigorous calculation (Derrida and Flyvbjerg 1987b). Although it is not clear if these singularities have any observable effects, they may be deeply related to the general nature of a multivalley structure dominated by valleys with finite weight.

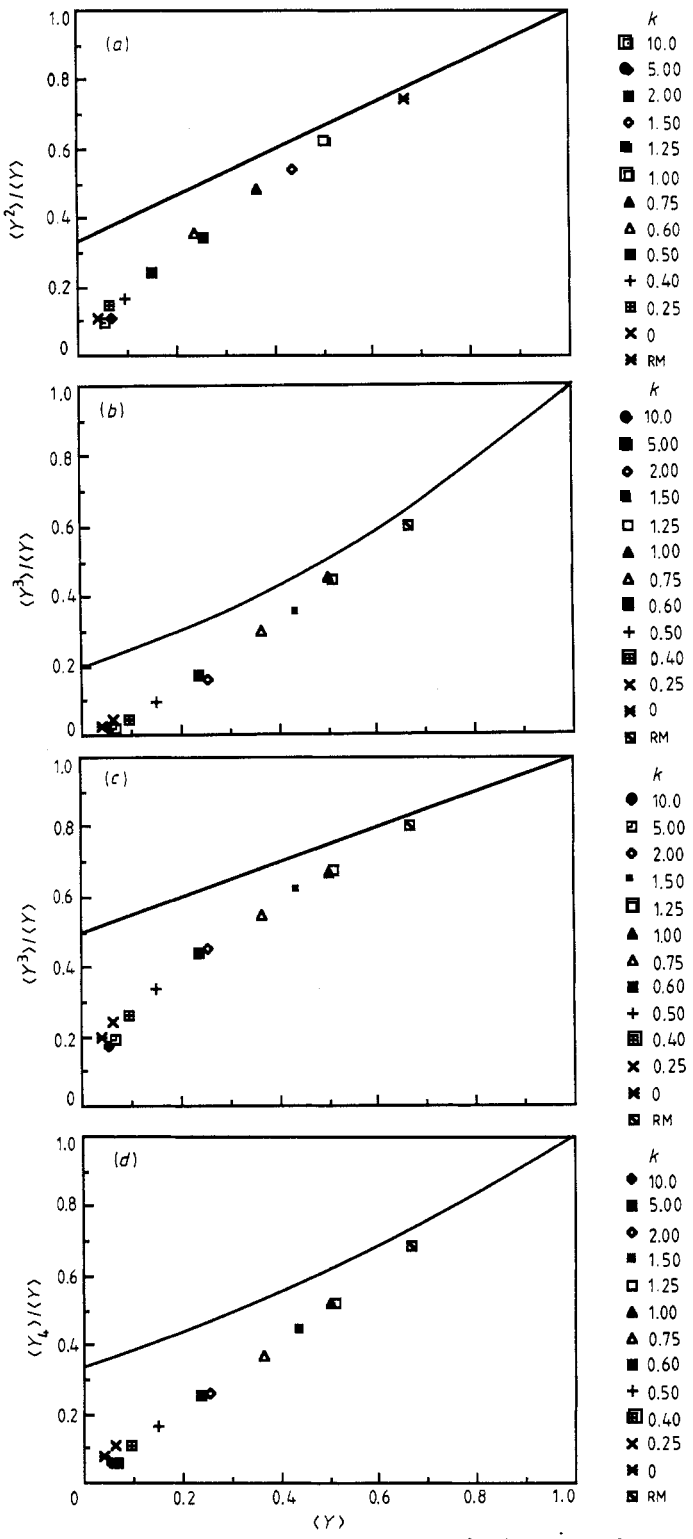

Figure 13. (*a*) A test of how well the relation $\langle Y^2\rangle = \frac{1}{3}(\langle Y\rangle + 2\langle Y\rangle^2)$ (full curve) is satisfied for different values of the asymmetry parameter k; see equation (4.4). Note that $\langle Y\rangle \equiv \langle Y_2\rangle$. (*b*) Same for relation $\langle Y^3\rangle = \frac{1}{15}(3\langle Y\rangle + 7\langle Y\rangle^2 + 5\langle Y\rangle^3)$, see equation (4.5). (*c*) Same for relation $\langle Y_3\rangle = \frac{1}{2}(\langle Y\rangle + \langle Y\rangle^2)$; see equation (4.6). (*d*) Same for relation $\langle Y_4\rangle = \frac{1}{6}(2\langle Y\rangle + 3\langle Y\rangle^2 + \langle Y\rangle^3)$; see equation (4.7).

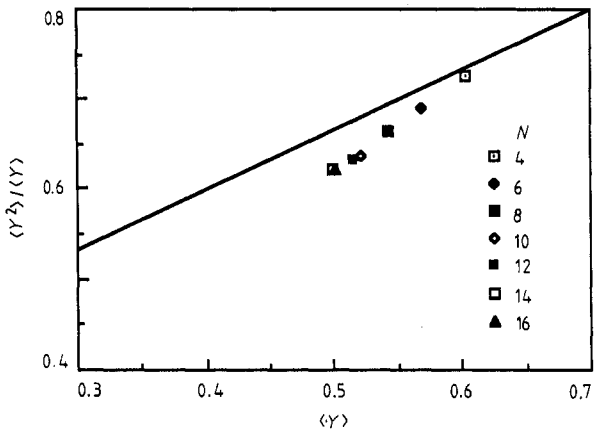

Figure 14. A test of the relation $\langle Y^2\rangle = \frac{1}{3}(\langle Y\rangle + 2\langle Y\rangle^2)$ for different sizes with parallel dynamics at $k = 1$.

We have calculated the function $\Pi(Y)$ in the model discussed in the present paper and investigated its k and size dependence. The results for $k = 1$, $N = 16$ are shown in figure 15 for parallel and sequential dynamics. The typical cusp-like singularities are clearly present. The behaviour is very different for $k < 0.5$. There $\Pi(Y)$ is concentrated around $Y = 0$ and the width narrows with increasing N, indicating that $\Pi(Y)$ will collapse into a δ function as $N \to \infty$. For $0.5 < k < 1$, we do find the cusp-like singularities, though there is also a strong N dependence and a significant shift of weight from higher to lower values of Y. This suggests that, for all $k < 1$, $\Pi(Y)$ will collapse to a δ function, though as $k \to 1$ this happens much more slowly with increasing N. The situation seems to be different for $k = 1$. Although, even in this case we find a very slight shift in $\Pi(Y)$ from higher to lower values, we believe that this is due to the fact that, for $N \leqslant 16$, $\langle Y\rangle$ did not yet converge to its limiting value. This should be compared to the random map model (§ 2.2), where we found that $\Pi(Y)$ is already independent of size at $N \simeq 10$.

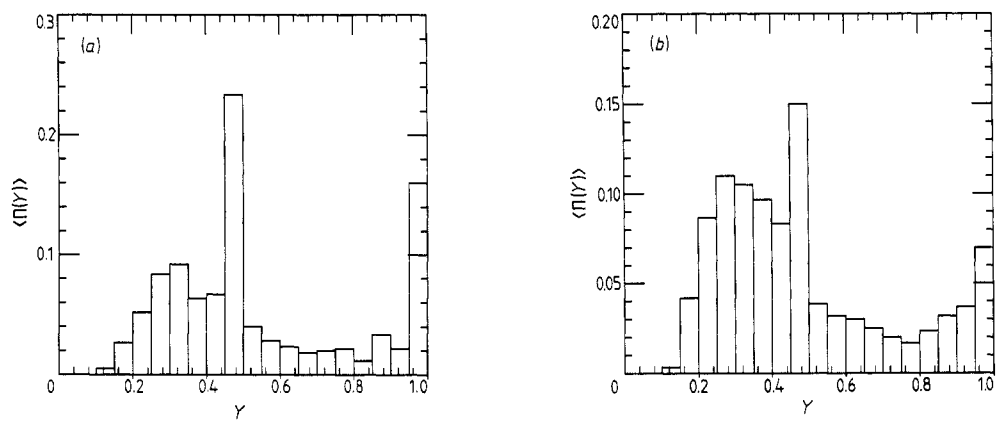

Figure 15. The probability distribution $\Pi(Y)$ for system size $N = 16$ and asymmetry parameter $k = 1$ with (a) sequential dynamics and (b) parallel dynamics.

To verify that $\langle Y \rangle$ actually converges to a finite limit as N increases, we have supplemented our analysis of small systems by applying the conventional method (mentioned in § 2) to calculate $\langle Y \rangle$ for larger systems. The N dependence of $\langle Y \rangle$ is shown in figure 16 for sequential dynamics. It seems fairly clear that $\langle Y \rangle$ is saturating to a value of about 0.45, for $k = 1$, but appears to vanish as $N \to \infty$ for $k = 0$ and $k = 0.5$.

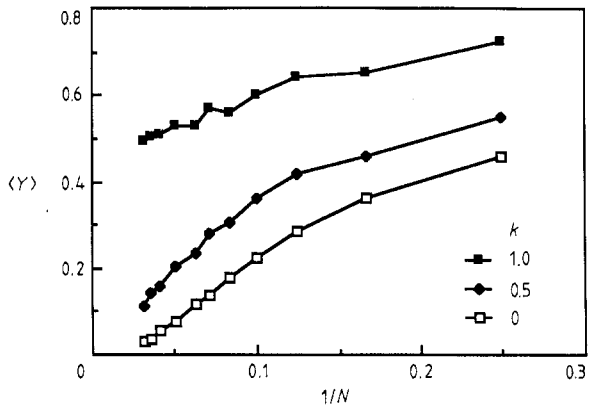

Figure 16. Size dependence of $\langle Y \rangle$ for different asymmetry parameter values. For $k = 1.0$ $\langle Y \rangle$ saturates to a value of about 0.45, whereas for $k = 0.5$ and $k = 0$ $\langle Y \rangle$ appears to tend to zero for $N \to \infty$.

5. Conclusions

We have studied in some detail the attractors of an asymmetric infinite-range Ising spin glass. Except for asymmetry parameter $k = 1$, the number of attractors increases exponentially with N and the dominant attractors are fixed points or limit cycles of short length, 2 or 4. At $k = 1$, however, the number of attractors is proportional to N and the average attractor size diverges, and a few attractors dominate. As a result, it is only for $k = 1$ that our model has a strong similarity to other models studied, such as the random map model and the infinite-range Ising spin glass with thermodynamic weighting of the attractors. The extent to which a few attractors dominate for $k = 1$ varies from sample to sample and is characterised by the distribution $\Pi(Y)$. As found for the other models (Derrida and Flyvbjerg 1987a, b) $\Pi(Y)$ has singularities at $Y = 1/n$, $n = 2, 3 \ldots$. It appears, then, that the dominance of a few basins is typical, provided that the number of attractors does not increase exponentially with N.

Acknowledgments

We would like to thank A J Bray and B Derrida for helpful discussions and H Sompolinsky for a critical reading of the manuscript. APY also thanks N Norris for interesting discussions on the work of Goles-Chacc *et al.* The work of JDR and APY is supported by the National Science Foundation under grants DMR 84-19536 and DMR 85-10593. We are also grateful to the Institute for Theoretical Physics in Santa Barbara, where this work was started, for hospitality. Work at Santa Barbara was

supported by the National Science Foundation through grant number PHY 82-17853, supplemented by funds from the National Aeronautics and Space Administration.

Appendix 1

Here we obtain the number of fixed points as a function of k following the lines of Tanaka and Edwards (1980). We start with equation (2.3), i.e.

$$\langle N_1(k)\rangle = \left\langle \mathrm{Tr} \int_0^\infty \prod_i \mathrm{d}\lambda_i \, \delta\left(\sum_j J_{ij}S_j - \lambda_i S_i\right)\right\rangle \tag{A1.1}$$

and use an integral representation for the delta function, i.e.

$$\langle N_1(k)\rangle = \left\langle \mathrm{Tr} \int_0^\infty \prod_i \mathrm{d}\lambda_i \int_{-\infty}^\infty \prod_i \left(\frac{\mathrm{d}x_i}{2\pi}\right) \right. \tag{A1.2}$$

$$\left. \times \exp\left(-\mathrm{i}\sum_i \lambda_i x_i S_i + \mathrm{i}\sum_{\langle i,j\rangle} [J_{ij}^{\mathrm{S}}(x_i S_j + x_j S_i) + J_{ij}^{\mathrm{A}}(x_i S_j - x_j S_i)]\right)\right\rangle.$$

Averaging over the J_{ij}, as described below equation (1.1), and making the replacement $x_i \to x_i S_i (1+k^2)^{1/2}/J$, $\lambda_i \to \lambda_i J/(1+k^2)^{1/2}$ one obtains

$$\langle N_1(k)\rangle = 2^N \int_0^\infty \prod_i \mathrm{d}\lambda_i \int_{-\infty}^\infty \prod_i \left(\frac{\mathrm{d}x_i}{2\pi}\right) \tag{A1.3}$$

$$\times \exp\left[-\mathrm{i}\sum_i \lambda_i x_i - \tfrac{1}{2}(1+k^2-2/N)\sum_i x_i^2 - \frac{(1-k^2)}{2N}\left(\sum_i x_i\right)^2\right].$$

Note that for $k=1$ the integrals decouple and are easily evaluated to give $\langle N_1(1)\rangle = 1$ (see equation (2.7)) for all N. For $k \neq 1$, one introduces an auxiliary variable to decouple the last term in equation (A1.3), which leads, with a simple change of variables, to

$$\langle N_1(k)\rangle = \left(\frac{N(1+k^2)-2}{2\pi(1+k^2)}\right)^{1/2} \int_{-\infty}^\infty \mathrm{d}\omega \, \exp\left(\frac{\omega^2}{1+k^2} - Nf(\omega)\right) \tag{A1.4}$$

where

$$f(\omega) = \tfrac{1}{2}\omega^2 - \ln I_k(\omega) \tag{A1.5}$$

and

$$I_k(\omega) = \int_{-\infty}^\infty \frac{\mathrm{d}x}{\pi} \int_0^\infty \mathrm{d}\lambda \, \exp\left\{-\tfrac{1}{2}x^2 + \mathrm{i}\left[\left(\frac{1-k^2}{1+k^2}\right)^{1/2}\omega - \lambda\right]x\right\}. \tag{A1.6}$$

Performing the x integral in equation (A1.5), $I_k(\omega)$ becomes

$$I_k(\omega) = \left(\frac{2}{\pi}\right)^{1/2} \int_0^\infty \mathrm{d}\lambda \, \exp\left\{-\tfrac{1}{2}\left[\lambda - \left(\frac{1-k^2}{1+k^2}\right)^{1/2}\omega\right]^2\right\} \tag{A1.7}$$

$$= 1 + \mathrm{erf}\left[\left(\frac{1-k^2}{2(1+k^2)}\right)^{1/2}\omega\right] \tag{A1.8}$$

where erf is the usual error function. Note that equation (A1.4) is exact, even for finite N, and can readily be evaluated numerically. For large N, one can do a steepest descent calculation with the result that

$$\langle N_1(k)\rangle = A(k)\exp(\alpha_1(k)N)[1+O(1/N)] \tag{A1.9}$$

where

$$\alpha_1(k) = -\tfrac{1}{2}\omega^{*2} + \ln I_k(\omega^*) \tag{A1.10}$$

and

$$A(k) = \exp[\omega^{*2}/(1+k^2)]/[f''(\omega^*)]^{1/2} \tag{A1.11}$$

where ω^* is the solution of

$$\omega^* = \left(\frac{2(1-k^2)}{\pi(1+k^2)}\right)^{1/2} \exp\left(-\frac{(1-k^2)}{2(1+k^2)}\omega^{*2}\right)\left\{1+\operatorname{erf}\left[\left(\frac{(1-k^2)}{2(1+k^2)}\right)^{1/2}\omega^*\right]\right\}^{-1}. \tag{A1.12}$$

These results were used in § 2. The expression for $\alpha_1(k)$ has also been derived by Sompolinsky (1987) and Bray (1987). Note that the error in the steepest descent formula, equation (A1.9) is small even for small sizes. For example, with $k=0$, where $\alpha_1(0)=0.1992$ and $A(0)=1.056$, equation (A1.9) predicts $\langle N_1(0)\rangle = 2.343$ for $N=4$, compared with the exact result $\langle N_1(0)\rangle = 2.396$, obtained by doing the integral in equation (A1.4).

Appendix 2

Computing the size of the different attractors and their basins of attraction is fairly easy. The states have labels m which run consecutively from 1 to 2^N, and each state has a 'basin number', n_m, which indicates the basin the state belongs to, and is initially set to zero for all states. For each state one computes the label of the state that is generated from it by the dynamics. These form a 2^N-dimensional array of 'next states'. This calculation is straightforward but turns out to be the most time-consuming part of the program. There is also a list of basin sizes, Ω_i, initially set to zero, for each basin i. One then performs the following steps starting with each state in turn.

Denote the label of the state by m and the number of basins that have already been found by i. Check whether state m has already been visited, by testing n_m. If it has been visited before ($n_m \neq 0$) skip to state $m+1$. If it has not ($n_m = 0$), then iterate the dynamics, labelling the states by basin number $i+1$, until you reach a state which has been visited before, and so has a basin number $n \neq 0$. There are now two possibilities, either (a) or (b), as follows.

(a) If $n = i+1$, this is then a new basin, so two steps need to be done:

(i) use the number of distinct states which have been visited since starting from state m, as a first estimate of Ω_{i+1}, and

(ii) determine the number of states on the $(i+1)$th attractor: the state just reached must be on the attractor, so note it and iterate the dynamics again counting the number of states until you come back to it again.

(b) If $n < i+1$, an old basin has been reached again. Go back to state m and iterate the dynamics again but this time label the states by basin number n. Count the number of distinct states visited until you hit a state already labelled to be on attractor n and add this number to Ω_n.

By the time that all states have been gone through in this way, each state is labelled by the number of the basin to which it belongs, and the size of each basin and its attractor have been determined.

References

Amit D J, Gutfreund H and Sompolinsky H 1987 *Ann. Phys., NY* **173** 30
Bray A J 1987 unpublished
Bray A J and Young A P 1987 unpublished
Crisanti A and Sompolinsky H 1987 *Preprint*
Derrida B and Flyvbjerg H 1986 *J. Phys. A: Math. Gen.* **19** L1003
—— 1987a *J. Physique* **48** 971
—— 1987b *J. Phys. A: Math. Gen.* **20** 5273
Derrida B and Toulouse G 1985 *J. Physique Lett.* **46** 223
Goles-Chacc E, Fogelman-Soulie F and Pellegrin D 1985 *Discr. Appl. Math.* **12** 261
Hertz J A, Grinstein G and Solla S A 1987 *Heidelberg Colloq. on Glassy Dynamics* ed J L van Hemmen and I Morgenstern (Berlin: Springer) p 538
Hopfield J J 1982 *Proc. Natl Acad. Sci. USA* **79** 2554
Kirkpatrick S and Sherrington D 1978 *Phys. Rev.* **17** 4384
Kauffman S A 1969 *J. Theor. Biol.* **22** 437
—— 1984 *Physica* **10D** 145
Little W A 1974 *Math. Biosci.* **19** 101
Mézard M, Parisi G, Sourlas N, Toulouse G and Virasoro M 1984 *J. Physique* **45** 843
Mézard M, Parisi G and Virasoro M 1985 *J. Physique Lett.* **45** 217
Sherrington D and Kirkpatrick S 1975 *Phys. Rev. Lett.* **35** 1792
Sompolinsky H 1987 unpublished
Tanaka F and Edwards S F 1980 *J. Phys. F: Met. Phys.* **10** 2471